JOURNAL OF BACTERIOLOGY, Mar. 2008, p. 2086–2095 Vol. 190, No. 6
0021-9193/08/$08.00+0 doi:10.1128/JB.01678-07

The C-Terminal Extension of Ferrochelatase Is Critical for Enzyme Activity and for Functioning of the Tetrapyrrole Pathway in *Synechocystis* Strain PCC 6803▽†

Roman Sobotka,[1,2]* Samantha McLean,[3] Monika Zuberova,[4] C. Neil Hunter,[3] and Martin Tichy[1,2]

Institute of Microbiology, Department of Autotrophic Microorganisms, Opatovicky mlyn, 379 81 Trebon, Czech Republic[1]; Institute of Physical Biology, University of South Bohemia, 373 33 Nove Hrady, Czech Republic[2]; Department of Molecular Biology and Biotechnology, University of Sheffield, Firth Court, Sheffield S10 2TN, United Kingdom[3]; and Faculty of Science, University of South Bohemia, Branisovska 31, 370 05 Ceske Budejovice, Czech Republic[4]

Received 17 October 2007/Accepted 3 January 2008

Heme and chlorophyll (Chl) share a common biosynthetic pathway up to the branch point where magnesium chelatase and ferrochelatase (FeCH) insert either magnesium for Chl biosynthesis or ferrous iron for heme biosynthesis. A distinctive feature of FeCHs in cyanobacteria is their C-terminal extension, which forms a putative transmembrane segment containing a Chl-binding motif. We analyzed the ΔH324 strain of *Synechocystis* sp. strain PCC 6803, which contains a truncated FeCH enzyme lacking this C-terminal domain. Truncated FeCH was localized to the membrane fraction, suggesting that the C-terminal domain is not necessary for membrane association of the enzyme. Measurements of enzyme activity and complementation experiments revealed that the ΔH324 mutation dramatically reduced activity of the FeCH, which resulted in highly upregulated 5-aminolevulinic acid synthesis in the ΔH324 mutant, implying a direct role for heme in the regulation of flux through the pathway. Moreover, the ΔH324 mutant accumulated a large amount of protoporphyrin IX, and levels of Chl precursors were also significantly increased, suggesting that some, but not all, of the "extra" flux can be diverted down the Chl branch. Analysis of the recombinant full-length and truncated FeCHs demonstrated that the C-terminal extension is critical for activity of the FeCH and that it is strictly required for oligomerization of this enzyme. The observed changes in tetrapyrrole trafficking and the role of the C terminus in the functioning of FeCH are discussed.

In photosynthetic organisms, tetrapyrrole pigments such as heme and chlorophyll (Chl) are produced via a common branched pathway. The initial precursor, 5-aminolevulinic acid (ALA), is made in three steps from glutamate through glutamyl-tRNA and is subsequently converted via several steps into the metal-free tetrapyrrole ring, protoporphyrin IX (Proto), the last common precursor for both Chl and heme biosynthesis. At the branch point, Proto can act as a substrate for either ferrochelatase (FeCH), which catalyzes the insertion of ferrous iron forming heme, or for magnesium chelatase, which inserts Mg^{2+} to produce the first Chl biosynthetic intermediate, Mg-Proto (Fig. 1A) (for reviews, see references 1 and 37).

Because the levels of heme and Chl vary according to cell development, growth, or light conditions, special regulatory mechanisms have evolved which control heme and Chl formation and coordinate their levels with the synthesis of the corresponding apoproteins (23, 37). Stringent control of this pathway is particularly essential for oxygenic organisms such as plants and cyanobacteria that have to cope with the problem of photooxidation. Chl, as well as its intermediates, is readily excited by light and, unquenched, forms destructive oxygen species under aerobic conditions. Therefore, for organisms carrying out oxygenic photosynthesis, it is essential to minimize cellular levels of unbound, free tetrapyrroles.

Although the enzymatic steps of tetrapyrrole synthesis from glutamate to Chl and heme are almost completely elucidated at the genetic level (37), current knowledge of the regulation and biochemistry of tetrapyrrole metabolism is still lacking. ALA synthesis was established as the rate-limiting step that determines the total flux through the pathway (1, 37), and this step appears to be feedback inhibited by heme (Fig. 1A) (1, 37). Also, insertion of the particular metal is expected to be an important regulatory step, manifested as a tightly controlled distribution of Proto between the Mg and Fe chelatases (4, 27, 44). Expression levels and/or activities of these chelatases are apparently controlled by light, diurnal and circadian rhythmicity (20, 26). In higher plants the activities of both chelatases oscillate with almost inverse amplitude when plants are grown in cycles of 12 h of light/12 h of dark (26). Although this can explain diurnal alteration of Proto distribution to the Chl branch during daytime and to heme at night, the precise mechanism that ultimately controls the unequal distribution of Proto between both pathways remains unclear.

FeCH is an enzyme of special interest regarding regulation of tetrapyrrole biosynthesis. FeCH activity may regulate the flux down both the heme and Chl branches of the pathway via increased production of heme, which then exerts feedback control by inhibiting synthesis of ALA at the start of the pathway (1, 34). It might also control the direction of Proto at the Chl/heme branch point by differential consumption of this

* Corresponding author. Mailing address: Institute of Microbiology, Department of Autotrophic Microorganisms, Opatovicky mlyn, 379 81 Trebon, Czech Republic. Phone: 42 384 340434. Fax: 42 384 340415. E-mail: sobotka@alga.cz.

† Supplemental material for this article may be found at http://jb.asm.org/.

▽ Published ahead of print on 11 January 2008.

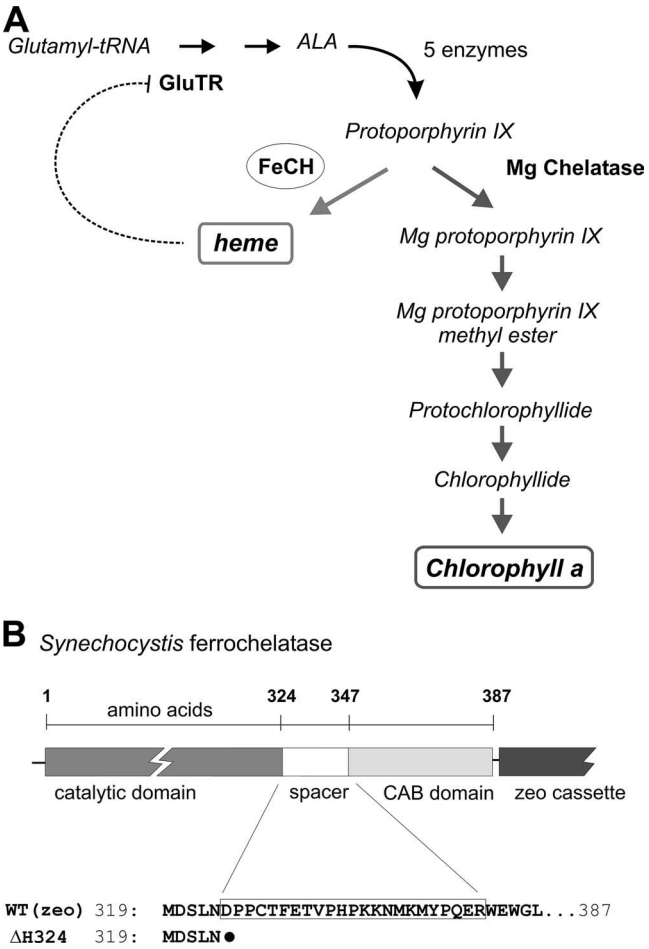

FIG. 1. (A) The tetrapyrrole biosynthetic pathway in cyanobacteria. FeCH (circled) lies at the branch point between heme and Chl biosynthesis, sharing the same substrate Proto with the magnesium chelatase. The positions of the Chl precursors relevant for this study are also shown. This model of pathway regulation (reviewed in references 1 and 37) proposes that activity of the glutamyl-tRNA reductase (GluTR) at the beginning of the pathway is inhibited by heme (dotted line), which in turn controls synthesis of the ALA and ultimately the total flux through the pathway. (B) Schematic presentation of the *Synechocystis* FeCH with catalytic and C-terminal CAB domains connected by a spacer. The position of the zeocin (zeo) resistance cassette is also indicated. Amino acid alignment of the FeCH C terminus shows the FeCH truncation in the ΔH324 strain; the black dot indicates a stop codon.

common substrate (33, 44). We have recently demonstrated that FeCH activity is involved in the regulation of Chl biosynthesis, as decreased activity of this enzyme was followed by a substantial increase in the level of Chl precursors and in the accumulation of Chl (33).

An intriguing feature of FeCH from cyanobacterial and chloroplast sources is the hydrophobic C-terminal extension with a putative Chl-binding motif (CAB domain). This highly conserved CAB domain is connected to the FeCH catalytic core by a more variable spacer (see Fig. S1 in the supplemental material); however, the functions of the spacer and CAB domains are not known.

The data reported herein show that the C-terminal extension of the FeCH of the cyanobacterium *Synechocystis* sp. strain PCC 6803 is essential for accumulation and activity of FeCH in the cell. We have found that although the C terminus is not the sole determinant of membrane binding of the FeCH, deletion of this segment dramatically reduces FeCH activity both in vivo and in vitro and leads to dramatic changes in tetrapyrrole biosynthesis. Importantly, analysis of the recombinant full-length and truncated FeCHs demonstrated that the C-terminal extension is essential for oligomerization of the enzyme. The significance of these data for the function of FeCH and regulation of tetrapyrrole metabolism in cyanobacteria is discussed.

MATERIALS AND METHODS

Growth conditions. Cells of *Synechocystis* strain PCC 6803 were grown photoautotrophically in liquid BG-11 medium (31) supplemented by 10 mM TES [*N*-tris(hydroxymethyl)methyl-2-aminoethanesulfonic acid] at 30°C and 30 μmol of photons m^{-2} s^{-1} (normal light) on a rotary shaker.

Construction of mutants of *Synechocystis* strain PCC 6803. The C1.8 mutant strain carrying a short deletion in the Chl-binding CP47 protein was previously constructed by Tichy and Vermaas (38). The ΔH324 mutant was constructed in several steps. First, a zeocin resistance cassette was placed immediately behind the *hemH* gene by PCR-mediated insertion (18). Second, DNA from the resulting WT_{zeo} (where WT is wild type) strain was isolated and used as the template for site-directed mutagenesis based on the PCR megaprimer method (15). A PCR product was prepared containing the *hemH* gene with a stop codon introduced at amino acid position 324, the zeocin cassette, and corresponding upstream and downstream regions. This PCR product was directly used to transform the WT to prepare the ΔH324 strain. *Synechocystis* transformants were selected on medium with increasing amounts of zeocin (3 to 24 mg $liter^{-1}$). Oligonucleotides used for mutagenesis are described in Table S1 in the supplemental material.

Fractionating of *Synechocystis* cells. A total of 50 ml of cells (an optical density at 750 nm [OD_{750}] of ~ 0.5) were washed and resuspended in the thylakoid buffer containing 20 mM HEPES, pH 7.4, 10 mM $MgCl_2$, 5 mM $CaCl_2$, and 20% glycerol. The cell suspension was mixed with glass beads and broken in a MiniBeadBeater, and the resulting homogenate was divided into halves. To prepare a whole-cell extract, the first part was solubilized by 1% β-dodecyl-maltoside and centrifuged at 32,000 × *g* for 10 min at 4°C to discard unbroken cells. The second part was centrifuged at 100,000 × *g* for 30 min at 4°C, and the supernatant containing soluble proteins was transferred to a new tube. Pelleted membranes were washed in thylakoid buffer and suspended in the same buffer containing 1% β-dodecyl-maltoside, and unbroken cells were discarded by centrifugation.

Western blotting and immunoblotting. Unless otherwise stated, soluble or membrane proteins were denatured by 2% sodium dodecyl sulfate (SDS) and 2% dithiothreitol for 30 min at room temperature and separated by SDS-polyacrylamide gel electrophoresis (PAGE) in a denaturing 12 to 20% linear-gradient polyacrylamide gel containing 7 M urea (16). Proteins separated in the gel were transferred onto a polyvinylidene difluoride membrane. The membrane was incubated with specific primary antibodies and then with secondary antibody-horseradish peroxidase conjugate (Sigma, Germany). The anti-FeCH antibody kindly provided by Annegret Wilde (Humbold University, Germany) was raised in rabbits against recombinant *Synechocystis* glutathione *S*-transferase-FeCH prepared in *Escherichia coli*. To examine the association of FeCH with membranes, the isolated membranes were treated with 2 M NaCl in 0.1 M CAPS [3-(cyclohexylamino)-1-propanesulfonic acid; pH 11.0] or 0.1 M Na_2NO_3 for 30 min at 4°C and pelleted by centrifugation. The washed membranes were resuspended in thylakoid buffer (described above) and separated by SDS-PAGE.

FeCH activity assay. FeCH activity was monitored spectrofluorometrically at 35°C by directly recording the rate of zinc-Proto formation using a Spectronic Unicam series 2 spectrofluorometer (3). The reaction mixture (1.5-ml final volume) contained 0.3 M Tris-HCl (pH 8.0), 0.03% Tween 80, 2 μM Proto, and 1.5 μM $ZnSO_4$. The measurement of *Synechocystis* native FeCH was initiated by adding proteins in amounts corresponding to 0.3 ml of cells at an OD_{730} of 1. This value was calculated from the Chl content in the analyzed sample and Chl level per OD_{730} unit of the particular strain. Recombinant FeCHs were assayed by adding of 5 μg of solubilized *E. coli* membranes into the reaction mixture.

Quantification of Chl and its intermediates. Chl was extracted from cell pellets (10 ml; OD_{730} of ~0.5) with 100% methanol, and its content was measured spectrophotometrically (29).

For quantitative determination of Chl precursors in the cells, 100 ml of culture

at an OD_{730} of ~0.4 was filtered through a 4-μm-pore-size cellulose filter to remove all precipitated pigments in the growth medium and harvested. Cells were extracted by 1 ml of alkaline acetone (acetone–0.1 N ammonium hydroxide; 9:1, vol/vol) using a Mini-BeadBeater with six breaking cycles. Subsequently, the sample was centrifuged, and the supernatant containing extracted pigments was collected. The pellet was then extracted twice by 1 ml of alkaline acetone with one breaking cycle. Combined supernatants were extracted once by an equal volume of hexane to remove Chl and immediately subjected to high-performance liquid chromatography analysis with a Vydac 201TP54 column (250 mm by 4.6 mm; C_{18} reverse-phase silica gel). The tetrapyrroles were quantified essentially as described previously (33).

Analysis of pigments in growth medium. For quantification of Proto precipitated in growth medium, a 4-μm-pore-size cellulose filter (see the previous paragraph) was frozen in liquid nitrogen, powdered in a 2-ml Eppendorf tube, and dissolved in 0.5 ml of alkaline acetone. Acetone was then extracted with 250 μl of hexane to remove Chl. Proto was diluted in 20 ml of 0.1 M KOH–0.03% Tween 80 and quantified spectroscopically using an authentic standard (Sigma, Germany). To determine pigments dissolved in growth medium, 100 ml of culture was filtered through a 0.22-μm-pore-size filter to remove cells. The filtrate was loaded onto an Oasis HLB extraction cartridge (Waters), and bound pigments were eluted with 1 ml of methanol and analyzed spectroscopically.

Determination of ALA-synthesizing capacity. A total of 100 ml of *Synechocystis* cells at an OD_{730} of 0.4 were supplemented with 3 mM levulinic acid to inhibit ALA condensation into porphobilinogen. After 2 h cells were harvested, resuspended in 0.3 ml of double-distilled H_2O, and mixed with 20 μl of 50% trichloroacetic acid. Precipitated proteins were discarded by centrifugation, and the supernatant was adjusted to pH 6.7 by 90 μl of 0.5 M Na_3PO_4. The supernatant was then mixed with 20 μl of ethylacetoacetate, boiled for 15 min at 100°C, and cooled on ice. A total of 400 μl of modified Ehrlich's reagent was added to the supernatant, and ALA accumulation was determined by absorption at 553 nm (21).

Cloning and expression of WT and truncated FeCH in *E. coli*. The *Synechocystis hemH* gene was amplified by PCR using gene-specific oligonucleotides and *Synechocystis* genomic DNA as a template. The resulting PCR product was cloned into the pET9a-His_6 vector (14). Oligonucleotides were used to insert a stop codon into the *Synechocystis hemH* gene at amino acid position 324 using the pET9a-His_6-*hemH* vector as a template and QuickChange site-directed mutagenesis (Stratagene). pET9a-His_6-*hemH* and pET9a-His_6-ΔH324 plasmids were transformed into *E. coli* BL21(DE3) cells. The cultures were induced overnight at 20°C using 0.4 mM isopropyl-β-D-thiogalactopyranoside. About 10 colonies from each transformation were monitored for protein expression by SDS-PAGE, and those accumulating comparable amounts of each recombinant FeCH per cell were used for further experiments.

Preparation and solubilization of *E. coli* membrane proteins. A total of 100 ml of induced cells (OD_{600}s of 2 to 3) were washed and resuspended in the buffer containing morpholineethanesulfonic acid-KOH (pH 6.1), 10 mM $MgCl_2$, 5 mM $CaCl_2$, 20% glycerol, and 0.2 mM Tris(2-carboxyethyl)phosphine. The cell suspension was broken in a Mini-BeadBeater, and the resulting homogenate was centrifuged at 32,000 × *g* for 20 min at 4°C to pellet membranes. Membranes were solubilized for 30 min at room temperature in 0.5 ml of the same buffer with 2% β-dodecyl-maltoside and centrifuged to discard cell debris. Total protein in the sample was quantified by a bicinchoninic protein assay kit (reducing agent compatible; Pierce) and adjusted to 1 μg/μl.

Purification of the recombinant FeCHs and determination of their aggregation states. A mixture of 300 mM NaCl and 10 mM imidazole was added to the *E. coli* membranes solubilized in the thylakoid buffer as described above. This solution was filtered through a 0.22-μm-pore-size filter and loaded onto a Proteus immobilized metal affinity chromatography mini-column (Pro-Chem) equilibrated with thylakoid buffer containing 0.3 M NaCl, 10 mM imidazole, and 0.1% β-dodecyl-maltoside. The resin was washed with the same buffer containing 35 mM imidazole, and the recombinant His_6-tagged FeCH was eluted with thylakoid buffer containing 200 mM imidazole and 0.5% β-dodecyl-maltoside. Nondenaturing PAGE was performed with a precast 4 to 16% native PAGE bis-Tris gel system (Invitrogen) at 10 V/cm at 4°C. A total of 0.5 μg of protein in the thylakoid buffer was loaded for each sample, and after the electrophoresis the gel was stained with Coomassie brilliant blue.

Gel filtration chromatography was carried out on a BioSep SEC-S3000 300- by 7.80-mm column (Phenomenex) connected to a Waters 996 photodiode array detector (Waters, Milford, MA). The column was equilibrated with thylakoid buffer containing 0.1% β-dodecyl-maltoside. The flow rate was 0.2 ml/min.

TABLE 1. Growth rate and Chl content of mutant and wild-type strains of *Synechocystis* strain PCC 6803

Strain	Doubling time (h)[a]	Chl content (mg/liter/OD_{730} unit)
WT_{zeo}	13 ± 0.5	4.5 ± 0.15
ΔH324	23 ± 0.5	3.3–6.5[b]
$C1.8_{zeo}$	67 ± 2	3.8 ± 0.15
C1.8/ΔH324	19 ± 0.5	6.6 ± 0.25[c]

[a] Photoautotrophic growth at 30 μmol of photons m^{-2} s^{-1}.
[b] As shown in Fig. 2A.
[c] At an OD_{730} of ~0.4.

RESULTS

Phenotype of the ΔH324 mutant of *Synechocystis* strain PCC 6803. In the genome of the cyanobacterium *Synechocystis*, there is only one recognizable gene for FeCH, *hemH*, which has a strong similarity to algal and plant genes coding for FeCH, including the hydrophobic C-terminal region, within which there is a CAB domain (Fig. 1B; see also Fig. S1 in the supplemental material). In order to provide information regarding the function of this C-terminal extension of FeCH, we prepared mutant ΔH324 with a stop codon introduced at position 324, which approximates to the termination point in the soluble FeCH from *Bacillus subtilis* (Fig. 1B). To construct this strain, we first introduced a gene encoding zeocin resistance, yielding the strain WT_{zeo}, and in the next step we used DNA from WT_{zeo} as a template to prepare the ΔH324 mutant using megaprimer PCR site-directed mutagenesis (15).

The resulting ΔH324 mutant grew poorly (Table 1) and excreted large quantities of a red-brown compound that precipitated in the medium (see below). The time course of Chl accumulation during growth of ΔH324 in liquid culture was unusual. At low cell densities, accumulation of Chl in the cell was substantially higher than in the WT, whereas at higher ODs (>0.5) the Chl content per cell rapidly decreased (Fig. 2A). This loss of Chl is probably related to a decrease in light tolerance of this strain and accumulation of tetrapyrroles in cells (Fig. 2B) (see below). ΔH324 was unable to grow at a light intensity of 500 μmol of photons s^{-1} m^{-2} (see Fig. S2 in the supplemental material) and was two times more sensitive to fluridone, an inhibitor of carotenoid biosynthesis (5), than the WT, suggesting that the light sensitivity of ΔH324 is caused by photooxidative damage (see Fig. S2 in the supplemental material]).

It should be noted that introduction of the gene for zeocin resistance had no effect on either autotrophic growth or Chl accumulation (Table 1).

Analysis of tetrapyrrole metabolism. We showed previously that FeCH modulates accumulation of tetrapyrroles, which are known to mediate increased sensitivity to oxidative stress (33). To determine the effect of C-terminal truncation of FeCH on the Chl/heme biosynthetic pathway, levels of Proto, Mg-Proto monomethyl ester (Mg-PME), protochlorophyllide (PChlide), and chlorophyllide (Chlide) were quantified in the strains studied in the present work. Cells were grown under normal light conditions and harvested at an OD_{730} of ~0.4, at which point the ΔH324 strain still accumulates normal amounts of Chl. In the control WT_{zeo} strain, levels of Chl precursors were two to three times higher than in the WT, suggesting that insertion of

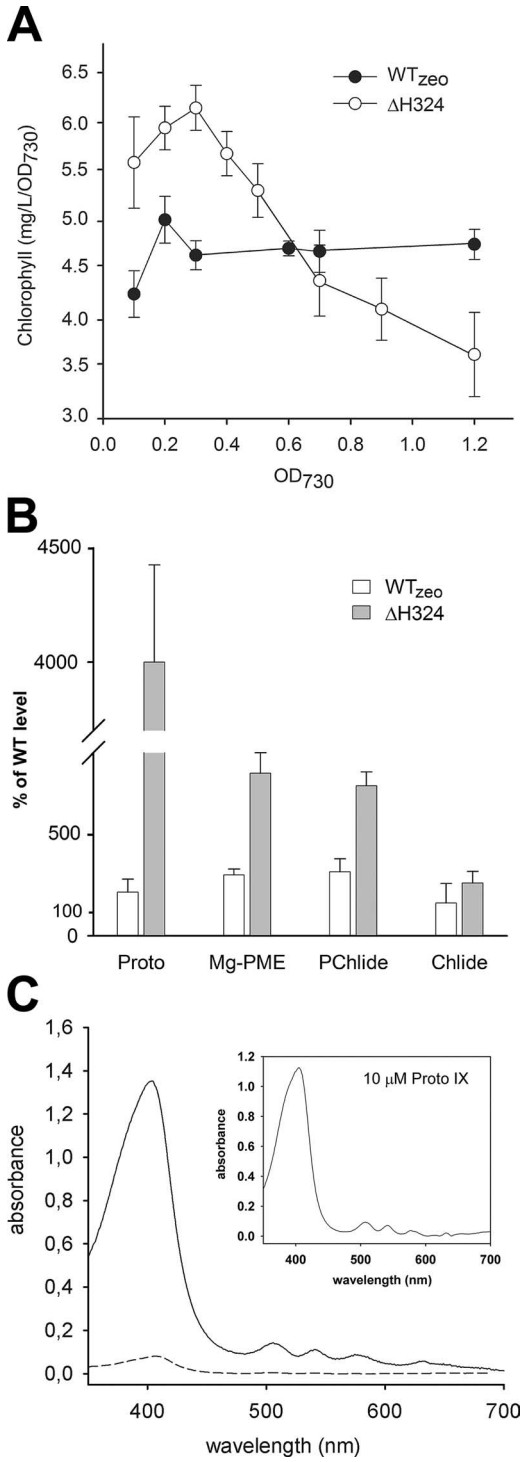

FIG. 2. Analysis of pigments in WT and mutants of *Synechocystis* strain PCC 6803. (A) Chl accumulation in *Synechocystis* strains during photoautotrophic growth. Data shown are from three experiments; the error bars indicate the standard deviation. (B) Quantification of the relative contents of Proto, Mg-PME, PChlide, and Chlide in *Synechocystis* cells harvested at an OD_{730} of 0.4. Chl precursors were extracted with alkaline acetone and quantified by a combination of high-performance liquid chromatography and spectrofluorometry. Values represent mean ± standard deviations from three separate extractions. (C) Absorbance spectra of the precipitate isolated from the growth medium of ΔH324 (solid line) and WT_{zeo} (short dash). The WT accumulated undetectable amounts of Proto. The inset shows the absorbance of 10 μM Proto standard diluted in the same solution.

the zeocin cassette 3′ to the *hemH* gene affects tetrapyrrole biosynthesis (Fig. 2B). However, a much higher accumulation of Proto was detected in the ΔH324 mutant, reaching a level ~45-fold higher than in WT, and levels of Mg-PME and PChlide were also very high (Fig. 2B).

As indicated above, the ΔH324 cells released a red-brown precipitate into the growth medium. This precipitate was separated from the cells and medium by filtration through 4-μm-pore-size filter, and spectroscopic analysis showed that this precipitate is almost pure Proto (Fig. 2C). The extent of accumulation of this pigment in the growth medium of ΔH324 was surprising; we estimated that 1 liter of growth medium from cells grown to a density of ~0.4 (OD_{730}) contained about 1.9 mg of Proto, which corresponds to almost half of the cellular Chl content. Small amounts of precipitated Proto were also found in the growth medium of WT_{zeo} (Fig. 2C), which correlates with the increased accumulation of Proto in ΔH324 and WT_{zeo} cells. No other tetrapyrrole intermediates except Proto were precipitated or dissolved in the growth medium of any of the strains studied.

To explain this substantial accumulation of Proto in ΔH324, the rate of ALA synthesis was assayed, since it is generally accepted as the key control point for the whole tetrapyrrole pathway and since increased ALA supply induces accumulation of tetrapyrroles (1). Importantly, we found that in the ΔH324 strain, the rate of ALA synthesis increased approximately fivefold in comparison with the WT or WT_{zeo} (ΔH324, 1,074 ± 72; WT, 219 ± 47; and WT_{zeo}, 247 ± 29 μmol of ALA per liter of cells at an OD_{730}).

To summarize, the truncation of FeCH resulted in a strain suffering strongly from photooxidative stress as a consequence of disturbed tetrapyrrole biosynthesis and accumulation of phototoxic intermediates of this pathway.

Localization, accumulation, and activity of FeCHs. Based on homology with light-harvesting complex (LHC) proteins, the FeCH C-terminal sequence may form a transmembrane segment containing a CAB domain. Deletion of this segment could lead to altered activity, localization, and/or destabilization of FeCH, affecting tetrapyrrole metabolism in ΔH324 mutants.

First, we addressed the localization of *Synechocystis* FeCH. Isolated WT membranes were treated with 2 M NaCl in 0.1 M CAPS (pH 11) or 0.1 M Na_2NO_3, salts known to remove extrinsic membrane proteins (2). After the salt treatment FeCH remained associated with the membrane, demonstrating that the full-length enzyme is anchored to the membrane by a putative helical segment (Fig. 3A).

To assess localization and accumulation of truncated FeCH, a whole-cell extract of the ΔH324 mutant was fractionated into cytosolic and membrane fractions, which were separated by SDS-PAGE, and blotted, and FeCH was detected by antibodies. The truncated FeCH exhibited the expected molecular mass of 38 kDa, and it was evident that the mutation significantly impaired accumulation of the enzyme, resulting in levels approximately 10% of the WT (Fig. 3B). In the whole-cell extract of the ΔH324 truncation mutant, another faint band with a molecular mass slightly greater than WT FeCH can be observed (Fig. 3B, highlighted by a black triangle). However, this band is very probably an unspecific cross-reaction of the anti-FeCH antibody with a soluble protein as it is also visible in

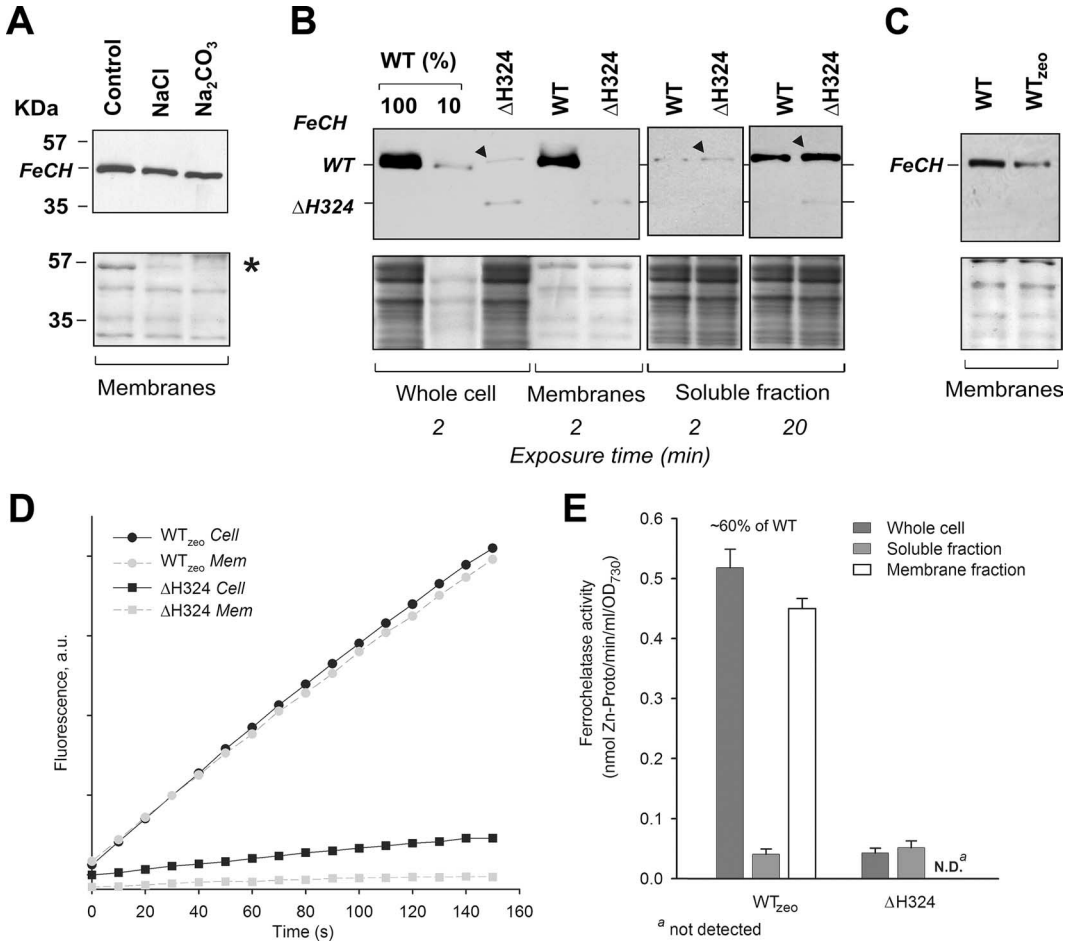

FIG. 3. Localization, accumulation, and in vitro activity of FeCH in *Synechocystis* strains. (A) Membranes prepared from the WT strain were washed with 2 M NaCl, pH 11, or 0.1 M Na_2CO_3 and centrifuged, and the pellet was separated by SDS-PAGE, blotted, and cross-reacted with anti-FeCH antibody. The lower panel shows the membrane stained with Ponceau red as a loading control; the peripheral subunit of ATPase, included as a marker protein for removal by salt washing, is indicated by an asterisk. (B) Whole-cell extract, membrane protein fraction, and soluble fraction from analyzed strains were prepared as described in Materials and Methods. The amount of protein loaded for each sample corresponded to 150 μl of cells at an OD_{730} of 1. FeCH was detected by an anti-FeCH antibody; the exposure time is indicated. The band resulting from an unspecific cross-reaction is marked by a black triangle. Below is the membrane stained with Ponceau red. (C) Different amounts of the FeCH in membrane fractions of the WT and WT_{zeo} strains. Samples were prepared, and the FeCH was detected as described above. (D) In vitro FeCH activity in whole-cell extract fractions (Cell; black symbols) and in membranes (Mem; gray symbols) as determined by continuous spectrofluorometric assay. Activities were monitored as an increase in fluorescence of zinc-Proto using excitation and emission wavelengths of 420 and 590 nm, respectively. (E) Comparison between FeCH activities measured in whole-cell extract, the soluble fraction, and the membrane fraction of studied strains. The values are the means of three independent experiments. au, arbitrary units.

the soluble fraction of both the WT and the truncated mutant but missing in the membrane fractions, where the FeCH is located (Fig. 3B). As shown in Fig. 3B, the truncated enzyme is located almost exclusively in the membrane fraction despite its lack of the putative transmembrane CAB domain. In the soluble fraction, no WT enzyme was found, and only a very weak signal was detectable for the ΔH324 FeCH after longer exposure of the Western blot (20 min versus 2 min) (Fig. 3B). The FeCH level also decreased to ~50% in the WT_{zeo} strain, suggesting that insertion of the resistance cassette influenced FeCH accumulation (Fig. 3C).

To compare the accumulation of FeCHs with their respective activities, FeCH was assayed in whole-cell extract and membrane and soluble fractions by spectrofluorometry using Proto and zinc as substrates. Consistent with the results of immunodetection, almost all FeCH activity in the WT was localized in membranes, and only traces of activity (<5%) were found in the soluble fraction, most probably as a contamination of the soluble fraction by nonsedimented membranes (Fig. 3D and E). In contrast, FeCH activity in the ΔH324 mutant reached 6% of WT, which would correspond to the decreased FeCH accumulation in the mutant. However, all the activity was localized in the soluble fraction (Fig. 3D and E) where only traces of FeCH were detected by immunoblotting (Fig. 3B). In agreement with FeCH immunodetection, the FeCH activity in the WT_{zeo} strain was reduced to 60% (Fig. 3E), which may be the reason for the accumulation of Chl precursors observed in this strain (Fig. 2B).

Assessment of the in vivo activity of truncated FeCH. Previous results (33) suggested that a decrease in in vitro FeCH

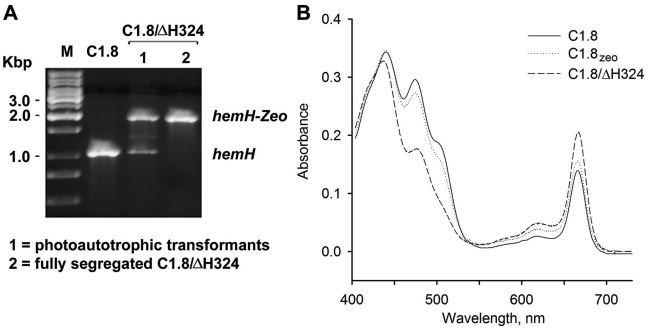

FIG. 4. Complementation of the C1.8 strain by the mutated ΔH324 *hemH* gene. (A) Segregation of the C1.8/ΔH324 mutant on the plate with no glucose (selection on autotrophy) and on the plate with 12 μl/ml of zeocine (fully segregated mutant). The *hemH* gene was amplified using total chromosomal DNA as a template; the mutant gene copy gave rise to a larger PCR fragment due to the insertion of the zeocin resistance cassette. (B) Absorbance spectra of methanol extracts from C1.8 mutants of *Synechocystis* strain PCC 6803. Pigments were extracted from the same volume of cells at an OD_{730} of ~ 0.4; Chl is represented by the 664-nm peak.

activity to a level similar to that found in the whole-cell extract of ΔH324 (~6% of WT) in the present work has a minimal effect on the *Synechocystis* phenotype and cannot explain the changes in tetrapyrrole metabolism observed in the ΔH324 mutant (Fig. 2). Moreover, there is a discrepancy in this strain between the very low FeCH activity found solely in the soluble fraction and the FeCH protein found mostly in the membrane fraction (Fig. 3).

To estimate the in vivo activity of FeCH, we employed an assay used previously to complement the C1.8 mutant of *Synechocystis* strain PCC 6803 (33). The C1.8 mutant, with a mutation in the Chl-binding CP47 protein, grows very slowly (Table 1), but its photosynthetic performance can be restored by spontaneous mutations in the *hemH* gene that reduce FeCH activity (31). The C1.8 strain is almost fully photoautotrophic when FeCH activity is reduced to a level which is 5 to 10% of WT (33; also, R. Sobotka, unpublished data). The reason this assay is effective for assaying for low FeCH activity in vivo is that, within limits, it is possible for *Synechocystis* to tolerate low FeCH activity, while at the same time lowered FeCH allows increased flux down the Chl branch to relieve problems in Chl synthesis. However, if FeCH activity is reduced even further, autotrophic growth is retarded.

For complementation, C1.8 was transformed by PCR fragments containing the mutated *hemH* gene from the ΔH324 strain, and autotrophic colonies were selected on medium with no glucose. Regarding the effect of the zeocin cassette on the FeCH activity, a $C1.8_{zeo}$ strain was prepared in order to create a proper control. As in the WT_{zeo} strain, the activity of FeCH in $C1.8_{zeo}$ was reduced by ~30%; nevertheless, as expected, this decrease was insufficient to increase the Chl level (by diverting flux down the Chl branch) (Fig. 1A) and improve the autotrophic growth rate of C1.8 (Table 1 and Fig. 4B).

Autotrophic transformants were repeatedly obtained for the ΔH324 transformations (data not shown). Interestingly, PCR analysis showed that autotrophic C.1.8/ΔH324 transformants were not fully segregated (they contained WT copies of *hemH*) even after cultures were restreaked several times onto new plates (Fig. 4A). The unsegregated strain had a doubling time of about 15 h, which is similar to the WT (Table 1), and did not accumulate Proto in the medium. This suggests that the C1.8/ΔH324 transformants can achieve optimal FeCH activity but only by keeping a copy, or copies, of the WT *hemH* gene. Indeed, the fully segregated C1.8/ΔH324 strain prepared by segregation on zeocin plates (Fig. 4A) grew more slowly than the unsegregated strain, and, as found for the ΔH324 mutant, it accumulated Chl (Table 1, Fig. 4B) and released significant quantities of Proto into the growth medium (result not shown).

This experiment showed clearly that the ΔH324 mutation very strongly affects the FeCH activity in vivo. Previous work has shown that no more than 5 to 10% of WT FeCH activity is required for normal growth of *Synechocystis* and that such a level is optimal for suppression of the C1.8 mutation (33). The fact that the fully segregated C1.8/ΔH324 strain grows more slowly than the unsegregated strain and also accumulates a significant level of Proto implies that the ΔH324 FeCH possesses very low ($\ll$5%) activity.

Activity and aggregation of recombinant FeCHs. To confirm that the C-terminal domain is required for the functioning of *Synechocystis* FeCH, recombinant full-length and truncated FeCHs were prepared in *E. coli* using the pET9a-His_6 vector (Novagen) and QuickChange mutagenesis (Stratagene).

Following induction of the *E. coli* strains, 46-kDa and 38-kDa polypeptides were produced that corresponded to the predicted sizes of full-length and truncated *Synechocystis* FeCHs, respectively (Fig. 5A). Accumulation levels of both recombinant enzymes were comparable, and each was detectable as a major species of the whole-cell extract, which allowed a simple comparison of their in vitro activities. Soluble and membrane fractions were prepared in a manner similar to that used for fractions from *Synechocystis* and, as in *Synechocystis*, both recombinant FeCHs were associated with the *E. coli* membranes (Fig. 5A).

Solubilized membrane fractions, each containing a similar amount of recombinant FeCH (Fig. 5A) (see Materials and Methods), were assayed for FeCH activity by the same method used for measurement of the *Synechocystis* enzyme. Whereas the enzymatic activity of recombinant WT FeCH was clearly detectable (Fig. 5B), the activity of the ΔH324 enzyme was at the detection limit of our assay (<2%) when 5 μg of membrane protein was assayed (Fig. 5B). We confirmed by a successful complementation of the Δ*hemH* strain of *E. coli* that the recombinant ΔH324 FeCH retains some residual activity (not shown). No indigenous FeCH activity was detected in a control sample prepared from *E. coli* transformed with an empty pET9a-His_6 plasmid (not shown), probably due to the fact that the assay conditions were optimized for the *Synechocystis* enzyme, and a small amount of total membrane protein was used for measurement.

For *Saccharomyces cerevisiae* and animal FeCHs, the homodimer has been shown to be the active form of the enzyme (11, 24). To elucidate the aggregation state of the *Synechocystis* enzymes, both WT and truncated recombinant FeCHs were purified by affinity chromatography from solubilized membranes (Fig. 6A), and their molecular sizes were determined. On a native gel WT FeCH migrates as two bands and partially as high-molecular-mass aggregates (>500 kDa). The mobilities of the observed bands are consistent with the sizes expected for

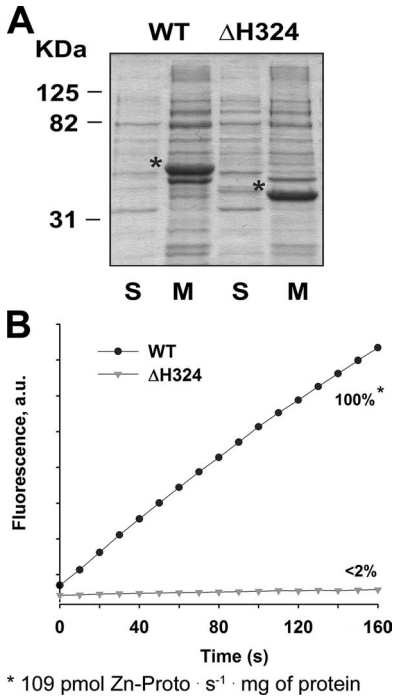

FIG. 5. Localization and activities of recombinant FeCHs. (A) Localization of recombinant WT and truncated FeCH overexpressed in *E. coli*. Five micrograms of soluble proteins (S) and 10 μg of membrane proteins (M), prepared from *E. coli* strains as described in Materials and Methods, were separated by SDS-PAGE, and the gel was stained with Coomassie brilliant blue. Recombinant FeCHs are marked by asterisks. (B) In vitro activity of recombinant FeCHs. Five micrograms of solubilized membranes, each containing a comparable amount of recombinant enzyme (as depicted in panel A) was assayed for FeCH activity essentially as described for *Synechocystis*. In three independent experiments including protein expression, the activity of the ΔH324 enzyme was always under the detectable threshold (<2%). au, arbitrary units.

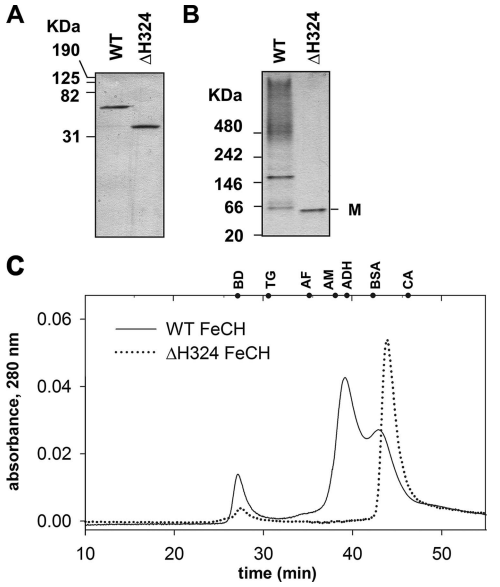

FIG. 6. Aggregation state of the recombinant FeCHs (A) A total of 0.5 μg each of the purified recombinant WT and truncated FeCH (ΔH324) was separated by 12% SDS-PAGE, and the gel was stained with Coomassie brilliant blue. (B) The same samples analyzed by nondenaturing PAGE. M indicates a position of FeCH monomer. (C) Gel filtration of the WT and truncated recombinant FeCH (ΔH324) on the BioSep SEC-S3000 column. Positions of standards are shown at the top of the graph. Standards are as follows: BD, blue dextran (void volume); TH, thyroglobulin (669 kDa); AF, apoferritin (443 kDa); AM, β-amylase (200 kDa); ADH, alcohol dehydrogenase (150 kDa); BSA, bovine serum albumin (66 kDa); CA, carbonic anhydrase (29 kDa).

monomeric and dimeric WT FeCHs, each with a detergent micelle (see below). In contrast, the truncated enzyme migrated to a position consistent only with a monomeric form (Fig. 6B).

When analyzed by gel filtration, WT FeCH migrated in two forms with different retention times; the major peak eluted at 39 min, which corresponds to an FeCH complex with a molecular mass of about 160 kDa. The second peak eluted at 42.5 min (~60 kDa), consistent with a monomeric FeCH (Fig. 6C). As the size of a β-dodecyl-maltoside micelle is 50 kDa (32), the molecular mass of observed FeCH complex is between a hypothetical dimer (140 kDa) and a trimer (185 kDa) covered by detergent. However, it is generally not simple to determine the masses of membrane proteins by gel filtration; calibration of the column with soluble proteins leads to inaccurate results (45). Truncated FeCH from the ΔH324 strain eluted only as a monomer with a predicted size of about 45 kDa (Fig. 6C). Given that the FeCH dimer has been described in other organisms (11, 24), we suggest that the FeCH oligomer shown on Fig. 6 is a homodimer, the formation of which strictly depends on the presence of the C-terminal extension.

DISCUSSION

In this study, we have investigated the function of the C-terminal extension of FeCH, a unique feature of this enzyme in photosynthetic organisms that has been preserved during evolution from cyanobacteria to higher plants. This region contains a putative CAB domain and a more variable spacer connecting the CAB domain with the catalytic core (see Fig. S1 in the supplemental material). It has been proposed that the function of the CAB domain is to direct FeCH to a specific membrane location within the chloroplast (39) and to anchor it there (13). It has also been hypothesized that FeCH is regulated through the binding of Chl to this domain (40). In contrast to plants, cyanobacteria do not contain multihelix CAB proteins such as LHC and related Chl binding peripheral antenna proteins, although genes coding for small single-helix CAB proteins have been found in genomes of many cyanobacteria (8). The *Synechocystis* genome encodes four small CAB-like Scp proteins sharing high sequence similarity to the FeCH CAB domain. Interestingly, Scp proteins appear to participate in regulation of tetrapyrrole biosynthesis (42), which might indicate a similar regulatory role for the FeCH C terminus.

In other groups of organisms the FeCH is also extended by characteristic forms of a C-terminal domain (see Fig. S1 in the supplemental material). In the mitochondrial FeCH and in FeCHs from some bacteria, this region contains cysteinyl ligands for a [2Fe-2S] cluster (7). Another distinct C terminus has been found in plant FeCH isoforms localized to nonpho-

tosynthetic tissue (36). The functions of these C-terminal domains also remain to be elucidated.

Our results suggest that the FeCH CAB domain forms an integral membrane segment, consistent with the results on green algae and plants (35, 39). However, using an enzyme truncated at the C terminus, we have demonstrated that this domain is not essential for membrane association. Thus, the truncated FeCH may resemble animal, yeast, and some bacterial FeCHs where an internal ~50-amino-acid segment at the N terminus was identified as being responsible for the membrane association (6, 10, 41). This hydrophobic segment, which is also the access route to the active site (41), is preserved in *Synechocystis* FeCH (see Fig. S1 in the supplemental material) and appears to be sufficient to maintain an association of FeCH with membrane as a peripheral protein.

The C terminus of FeCH is important for production of normal levels of this enzyme in the *Synechocystis* cell since its removal in the truncation mutant resulted in a level ~20% of the levels seen in the WT_{zeo} strain. As noted earlier, introduction of the zeocin cassette itself probably decreased the amount of FeCH by ~50%. (Fig. 3). Since we demonstrated that the recombinant full-length enzyme forms a complex, most probably a homodimer, via the C terminus (Fig. 6), it is likely that dimerization can stabilize FeCH in the *Synechocystis* cell. For yeast and animal FeCHs, the homodimer is the functional form of the enzyme required for stability (11, 24); and from the crystal structure of human FeCH, it is clear that the C-terminal extension promotes dimerization. The plastid FeCH probably also forms a homodimer (35). Moreover, dimerization of the FeCH CAB domain could arise from its high homology to two paired CAB helices within the structure of the LHC2 complex (19).

In contrast to yeast and animal FeCHs, where elimination of the C-terminal domain results in complete loss of activity (6), the truncated *Synechocystis* enzyme remained active as it is possible to prepare the fully segregated ΔH324 mutant and to use this truncated construct to complement the Δ*hemH* strain of *E. coli*. However, the membrane-bound FeCH of the ΔH324 strain functions dramatically less efficiently both in vivo and in vitro and in comparison with the full-length enzyme retains only traces (<2%) of activity. This was demonstrated by a high level of accumulation of Proto in the ΔH324 mutant of *Synechocystis* strain PCC 6803 and by rescue of photoautotrophic growth of the C1.8 mutant (Table 1). Furthermore, we did not find any in vitro activity of either native or recombinant ΔH324 FeCH associated with the cell membrane. We envision that, as in the case of yeast or animal FeCH, the homodimer is the fully active form of the *Synechocystis* FeCH. Moreover, as the dimerization of *Synechocystis* FeCH strictly depends on the presence of the C terminus with the CAB domain, it is tempting to speculate that the dimerization in vivo can be controlled via interaction with other CAB proteins, such as Scps, or with pigment molecules.

It is intriguing that it is possible to detect low activity of the FeCH in the soluble fractions (Fig. 3E) from *Synechocystis* even though the protein is almost undetectable by immunological methods. However, based on data from complementation of the C1.8 strain, in vitro activity of FeCH in the soluble fraction of the ΔH324 mutant is not relevant for the in vivo performance of the cell. *Synechocystis* possesses about 10 copies of its chromosome, and therefore unsegregated C1.8/ΔH324 cells with nine almost nonfunctional copies of the ΔH324 *hemH* gene could still "gain" ~10% of FeCH activity for optimal growth. This explains why the C1.8/ΔH324 mutant achieves the best possible growth rate by keeping a copy of the WT *hemH* gene (Fig. 4A). Moreover, we described previously two *Synechocystis* strains with point mutations in the catalytic domain of FeCH that cause a decrease in in vitro activity to 5 to 10% of the WT level with no apparent effect on phenotype (33).

The ΔH324 strain differs from a previously described $ScpA^-$ mutant of *Synechocystis* strain PCC 6803, where the *hemH* gene was interrupted by the kanamycin resistance cassette at position 332 (9). The $ScpA^-$ mutant grew as the WT and did not accumulate Proto. Interestingly, a light-sensitive strain with a deletion of photosystem I and carrying the $ScpA^-$ mutation was able to grow at normal light intensities (9), which is completely opposite to the phenotype of the ΔH324 mutant. It is therefore possible that the 8-amino-acid region missing in the ΔH324 FeCH but still present in the $ScpA^-$ enzyme is important for FeCH function. Unfortunately, the $ScpA^-$ FeCH possesses an extra 19-amino-acid segment at the C terminus, which arises from a frameshift of the kanamycin cassette, thus making interpretation of the $ScpA^-$ mutation problematic.

It is interesting that, despite the dramatic decrease in FeCH activity in the ΔH324 mutant, no depletion of phycobilisomes was observed that would indicate heme deficiency (Fig. S3). A similar "excess" of FeCH capacity in normally growing WT cells has been observed in other organisms: a 10-fold decrease in FeCH activity in the purple bacterium *Rhodobacter sphaeroides* or a 16-fold decrease in *B. subtilis* had no effect on cell viability (12, 25). Perhaps under nonstress conditions the majority of FeCH is not fully active in vivo; however, this deactivation is not detectable in an artificial in vitro assay.

In different groups of organisms, deficient FeCH activity leads to accumulation of Proto (10, 28, 43). In the ΔH324 mutant the accumulation of this compound is increased dramatically; ΔH324 cells excrete about 3.3 μmol/liter of Proto into the growth medium, compared to 90 μmol/liter in an *E. coli* strain metabolically engineered for the industrial production of Proto (17). It is not surprising that the growth of the ΔH324 mutant is impaired by light or by decreased carotenoid content (Fig. S2) as tetrapyrroles generally are readily excited by light and, unquenched, cause the formation of destructive radicals (43).

This uncontrolled accumulation of Proto in the ΔH324 strain can be explained by an almost fivefold increase in the rate of synthesis of the initial precursor ALA. Thus, our data support the model in which ALA synthesis and subsequent total metabolic flow through the tetrapyrrole pathway are controlled by heme availability (1). Heme probably interacts directly with the glutamyl-tRNA reductase, the first committed enzyme of the tetrapyrrole pathway, causing a decrease in its enzymatic activity (Fig. 1A) (30, 34).

The ΔH324 mutant accumulates significantly more Chl in the initial phase of growth than the WT (Fig. 2A), suggesting that a portion of the excess Proto can be metabolized by Mg chelatase. This is consistent with our recent discovery that Chl biosynthesis can be regulated by FeCH activity (33). In addi-

tion, introduction of the ΔH324 mutation into the C1.8 strain almost doubled cellular Chl content and rescued its photoautotrophic growth (Fig. 4B and Table 1). Further evidence supporting the regulatory role of FeCH has arisen from an analysis of the WT_{zeo} strain. Introduction of the zeocin cassette closely behind the *hemH* gene affected accumulation of FeCH, perhaps by destabilization of *hemH* mRNA. Nevertheless, only a 40% decrease in FeCH activity was followed by a threefold increase in the level of Chl precursors.

On the other hand, it is apparent that only a limited amount of overproduced Proto in ΔH324 is metabolized by the Chl branch, and the rest accumulates in the cell and is exported into the medium. This shows that the distribution of substrate between Fe and Mg chelatases is an important regulatory step in tetrapyrrole trafficking. Moreover, as the ΔH324 mutant accumulates PChlide but no Chlide (Fig. 2B), there might be an additional regulatory or feedback mechanism that operates within the Chl branch in a manner similar to that regulated by the FLU protein in higher plants (22).

ACKNOWLEDGMENTS

We thank Annegret Wilde for the antibody against the *Synechocystis* FeCH and Eva Prachova for her technical assistance.

R.S. and M.T. were supported by Institutional Research Concept no. AV0Z50200510 and by the project MSM6007665808 of the Ministry of Education of the Czech Republic. C.N.H. acknowledges financial support from the BBSRC (United Kingdom); S.M. was supported by a studentship from the University of Sheffield.

REFERENCES

1. **Beck, C. F., and B. Grimm.** 2006. Involvement of tetrapyrroles in cellular regulation, p. 223–235. *In* B. Grimm, R. J. Porra, W. Rüdiger, and H. Scheer (ed.), Chlorophylls and bacteriochlorophylls: biochemistry, biophysics, functions and applications. Advances in photosynthesis and respiration, vol. 25. Springer, Dordrecht, The Netherlands.
2. **Boudreau, E., Y. Takahashi, C. Lemieux, M. Turmel, and J. D. Rochaix.** 1997. The chloroplast ycf3 and ycf4 open reading frames of *Chlamydomonas reinhardtii* are required for the accumulation of the photosystem I complex. EMBO J. **16:**6095–6104.
3. **Camadro, J. M., and P. Labbe.** 1988. Purification and properties of ferrochelatase from the yeast *Saccharomyces cerevisiae*. Evidence for a precursor form of the protein. J. Biol. Chem. **263:**11675–11682.
4. **Castelfranco, P. A., and O. T. G. Jones.** 1975. Protoheme turnover and chlorophyll synthesis in greening barley tissue. Plant Physiol. **55:**485–490.
5. **Chamovitz, D., G. Sandmann, and J. Hirschberg.** 1993. Molecular and biochemical characterization of herbicide-resistant mutants of cyanobacteria reveals that phytoene desaturation is a rate-limiting step in carotenoid biosynthesis. J. Biol. Chem. **268:**17348–17353.
6. **Dailey, H. A., and T. A. Dailey.** 2003. Ferrochelatase, p. 93–121. *In* K. M. Kadish, K. M. Smith, and R. Guillard (ed.), The porphyrin handbook. Elsevier Science, St. Louis, MO.
7. **Dailey, T. A., and H. A. Dailey.** 2002. Identification of [2Fe-2S] clusters in microbial ferrochelatases. J. Bacteriol. **184:**2460–2464.
8. **Dolganov, N. A., D. Bhaya, and A. R. Grossman.** 1995. Cyanobacterial protein with similarity to the chlorophyll a/b binding proteins of higher plants: evolution and regulation. Proc. Natl. Acad. Sci. USA **92:**636–640.
9. **Funk, C., and W. Vermaas.** 1999. A cyanobacterial gene family coding for single-helix proteins resembling part of the light-harvesting proteins from higher plants. Biochem. **38:**9397–9404.
10. **Gora, M., J. Rytka, and R. Labbe-Bois.** 1999. Activity and cellular location in *Saccharomyces cerevisiae* of chimeric mouse/yeast and *Bacillus subtilis*/yeast ferrochelatases. Arch. Biochem. Biophys. **361:**231–240.
11. **Grzybowska, E., M. Gora, D. Plochocka, and J. Rytka.** 2002. *Saccharomyces cerevisiae* ferrochelatase forms a homodimer. Arch. Biochem. Biophys. **398:**170–178.
12. **Houghton, J. D., C. L. Honeybourne, K. M. Smith, H. D. Tabba, and O. T. G. Jones.** 1982. The use of N-methylprotoporphyrin dimethyl ester to inhibit ferrochelatase in *Rhodopseudomonas sphaeroides* and its effect in promoting biosynthesis of magnesium tetrapyrroles. Biochem. J. **208:**479–486.
13. **Jansson, S.** 1999. A guide to the *Lhc* genes and their relatives in *Arabidopsis*. Trends Plant Sci. **4:**236–240.
14. **Jensen, P. E., L. C. D. Gibson, K. W. Henningsen, and C. N. Hunter.** 1996. Expression of the *chlI*, *chlD* and *chlH* genes from the cyanobacterium *Synechocystis* PCC6803 in *Escherichia coli* and demonstration that the three cognate proteins are required for magnesium protoporphyrin chelatase activity. J. Biol. Chem. **271:**16662–16667.
15. **Ke, S.-H., and E. L. Madison.** 1997. Rapid and efficient site-directed mutagenesis by single-tube "megaprimer" PCR method. Nucleic Acid Res. **25:**3371–3372.
16. **Komenda, J., V. Reisinger, B. Ch. Müller, M. Dobakova, B. Granvogl, and L. A. Eichacker.** 2004. Accumulation of the D2 protein is a key regulatory step for assembly of the photosystem II reaction center complex in *Synechocystis* PCC 6803. J. Biol. Chem. **279:**48620–48629.
17. **Kwon, S. J., A. L. de Boer, R. Petri, and C. Schmidt-Dannert.** 2003. High-level production of porphyrins in metabolically engineered *Escherichia coli*: systematic extension of a pathway assembled from overexpressed genes involved in heme biosynthesis. Appl. Environ. Microbiol. **69:**4875–4883.
18. **Lee, J., H. J. Lee, M. K. Shin, and W. S. Ryu.** 2004. Versatile PCR-mediated insertion or deletion mutagenesis. BioTechniques **36:**398–399.
19. **Liu, Z., H. Yan, K. Wang, T. Kuang, J. Zhang, L. Gui, X. An, and W. Chang.** 2004. Crystal structure of spinach major light harvesting complex at 2.72Å resolution. Nature **428:**287–292.
20. **Matsumoto, F., T. Obayashi, Y. Sasaki-Sekimoto, H. Ohta, K. Takamiya, and T. Masuda.** 2004. Gene expression profiling of the tetrapyrrole metabolic pathway in *Arabidopsis* with a mini-array system. Plant Physiol. **135:**2379–2391.
21. **Mauzerall, D., and S. Granick.** 1956. The occurrence and determination of δ-aminolevulinic acid and porphobilinogen in urine. J. Biol. Chem. **219:**435–446.
22. **Meskauskiene, R., M. Nater, D. Goslings, F. Kessler, R. den Camp, and K. Apel.** 2001. FLU: a negative regulator of chlorophyll biosynthesis in *Arabidopsis thaliana*. Proc. Natl. Acad. Sci. USA **98:**12826–12831.
23. **Müller, B., and L. A. Eichacker.** 1999. Assembly of the D1 precursor in monomeric photosystem II reaction center precomplexes precedes chlorophyll *a*-triggered accumulation of reaction center II in barley etioplasts. Plant Cell **11:**2365–2377.
24. **Ohgari, Y., M. Sawamoto, M. Yamamoto, H. Kohno, and S. Taketani.** 2005. Ferrochelatase consisting of wild-type and mutated subunits from patients with a dominant-inherited disease, erythropoietic protoporphyria, is an active but unstable dimer. Hum. Mol. Genet. **14:**327–334.
25. **Olsson, U., A. Billberg, S. Sjövall, S. Al-Karadaghi, and M. Hansson.** 2002. In vivo and in vitro studies of *Bacillus subtilis* ferrochelatase mutants suggest substrate channeling in the heme biosynthesis pathway. J. Bacteriol. **184:**4018–4024.
26. **Papenbrock, J., H.-P. Mock, E. Kruse, and B. Grimm.** 1999. Expression studies in tetrapyrrole biosynthesis: inverse maxima of magnesium chelatase and ferrochelatase activity during cyclic photoperiods. Planta **208:**264–273.
27. **Papenbrock, J., H.-P. Mock, R. Tanaka, E. Kruse, and B. Grimm.** 2000. Role of magnesium chelatase activity in the early steps of the tetrapyrrole biosynthetic pathway. Plant Physiol. **122:**1161–1169.
28. **Papenbrock, J., S. Mishra, H. Mock, E. Kruse, E. Schmidt, A. Petersmann, H. Braun, and B. Grimm.** 2001. Impaired expression of the plastidic ferrochelatase by antisense RNA synthesis leads to a necrotic phenotype of transformed tobacco plants. Plant J. **28:**41–50.
29. **Porra, R. J., W. A. Thompson, and P. E. Kriedemann.** 1989. Determination of accurate extinction coefficients and simultaneous equations for assaying chlorophyll *a* and *b* extracted with four different solvents: verification of the concentration of chlorophyll standards by atomic absorption spectroscopy. Biochim. Biophys. Acta **975:**384–394.
30. **Rieble, S., and S. I. Beale.** 1991. Purification of glutamyl-transfer RNA reductase from *Synechocystis* sp. PCC 6803. J. Biol. Chem. **266:**9740–9745.
31. **Rippka, R., J. Deruelles, J. B. Waterbury, M. Herman, and R. Y. Stanier.** 1979. Generic assignments, strain histories and properties of pure cultures of cyanobacteria. J. Gen. Microbiol. **111:**1–61.
32. **Rosevear, P., T. VanAken, J. Baxter, and S. Ferguson-Miller.** 1980. Alkyl glycoside detergents: a simpler synthesis and their effects on kinetic and physical properties of cytochrome c oxidase. Biochemistry **19:**4108–4115.
33. **Sobotka, R., J. Komenda, L. Bumba, and M. Tichy.** 2005. Photosystem II assembly in CP47 mutant of *Synechocystis* sp. PCC 6803 is dependent on the level of chlorophyll precursors regulated by ferrochelatase. J. Biol. Chem. **280:**31595–31602.
34. **Srivastava, A., and S. I. Beale.** 2005. Glutamyl-tRNA reductase of *Chlorobium vibrioforme* is a dissociable homodimer that contains one tightly bound heme per subunit. J. Bacteriol. **187:**4444–4450.
35. **Suzuki, T., T. Masuda, D. P. Singh, F.-C. Tan, T. Tsuchiya, H. Shimada, H. Ohta, A. G. Smith, and K. Takamiya.** 2002. Two types of ferrochelatase in photosynthetic and nonphotosynthetic tissues of cucumber. J. Biol. Chem. **277:**4731–4737.
36. **Suzuki, T., T. Masuda, H. Inokuchi, H. Shimada, H. Ohta, and K. Takamiya.** 2000. Overexpression, enzymatic properties and tissue localization of a ferrochelatase of cucumber. Plant Cell Physiol. **41:**192–199.
37. **Tanaka, R., and A. Tanaka.** 2007. Tetrapyrrole biosynthesis in higher plants. Annu. Rev. Plant Biol. **58:**321–346.
38. **Tichy, M., and W. Vermaas.** 2000. Combinatorial mutagenesis and pseudor-

evertant analysis to characterize regions in loop E of the CP47 protein in *Synechocystis* sp. PCC 6803. Eur. J. Biochem. **267:**6296–6301.

39. **van Lis, R., A. Atteia, L. A. Nogaj, and S. I. Beale.** 2005. Subcellular localization and light-regulated expression of protoporphyrinogen IX oxidase and ferrochelatase in *Chlamydomonas reinhardtii*. Plant Physiol. **139:**1946–1958.
40. **Vavilin, D. V., and W. F. J. Vermaas.** 2002. Regulation of the tetrapyrrole biosynthetic pathway leading to heme and chlorophyll in plants and cyanobacteria. Physiol. Plant **115:**9–24.
41. **Wu, C. K., H. A. Dailey, J. P. Rose, A. Burden, V. M. Sellers, and B. C. Wang.** 2001. The 2-Å structure of human ferrochelatase, the terminal enzyme of heme biosynthesis. Nat. Struct. Biol. **8:**156–160.
42. **Xu, H., D. Vavilin, C. Funk, and W. Vermaas.** 2002. Small Cab-like proteins regulating tetrapyrrole biosynthesis in the cyanobacterium *Synechocystis* sp. PCC 6803. Plant Mol. Biol. **49:**149–160.
43. **Yang, H., H. Inokuchi, and J. Adler.** 1995. Phototaxis away from blue light by an *Escherichia coli* mutant accumulating protoporphyrin IX. Proc. Natl. Acad. Sci. USA **92:**7332–7336.
44. **Yaronskaya, E., V. Ziemann, G. Walter, N. Averina, T. Börner, and B. Grimm.** 2003. Metabolic control of the tetrapyrrole biosynthetic pathway for porphyrin distribution in the barley mutant *Albostrians*. Plant J. **35:**512–522.
45. **Zouni, A., J. Kern, J. Frank, T. Hellweg, J. Behlke, W. Saenger, and K. D. Irrgang.** 2005. Size determination of cyanobacterial and higher plant photosystem II by gel permeation chromatography, light scattering, and ultracentrifugation. Biochemistry **44:**4572–4581.